

Bound state vector solitons with locked and precessing states of polarization

Chengbo Mou, Sergey V. Sergeyev,* Aleksey G. Rozhin, and Sergei K. Turitsyn

Aston Institute of Photonic Technologies, School of Engineering & Applied Science Aston University, Birmingham, B4 7ET, UK

*s.sergeyev@aston.ac.uk

Abstract: We report experimental observation of new tightly and loosely bound state vector solitons with locked and precessing states of polarization in a carbon nanotube mode locked fiber laser in the anomalous dispersion regime.

©2013 Optical Society of America

OCIS codes: (060.3510) Lasers, fiber; (140.4050) Mode-locked lasers; (250.5530) Pulse propagation and temporal solitons.

References and links

1. B. C. Collings, S. T. Cundiff, N. N. Akhmediev, J. M. Soto-Crespo, K. Bergman, and W. H. Knox, "Polarization-locked temporal vector solitons in a fiber laser: experiment," *J. Opt. Soc. Am. B* **17**(3), 354–365 (2000).
2. S. T. Cundiff, B. C. Collings, N. N. Akhmediev, J. M. Soto-Crespo, K. Bergman, and W. H. Knox, "Observation of polarization-locked vector solitons in an optical fiber," *Phys. Rev. Lett.* **82**(20), 3988–3991 (1999).
3. J. H. Wong, K. Wu, H. H. Liu, C. M. Ouyang, H. H. Wang, S. Aditya, P. Shum, S. N. Fu, E. J. R. Kelleher, A. Chernov, and E. D. Obraztsova, "Vector solitons in a laser passively mode-locked by single-wall carbon nanotubes," *Opt. Commun.* **284**(7), 2007–2011 (2011).
4. L. M. Zhao, D. Y. Tang, H. Zhang, and X. Wu, "Polarization rotation locking of vector solitons in a fiber ring laser," *Opt. Express* **16**(14), 10053–10058 (2008).
5. T. Udem, R. Holzwarth, and T. W. Hänsch, "Optical frequency metrology," *Nature* **416**(6877), 233–237 (2002).
6. J. Mandon, G. Guelachvili, and N. Picque, "Fourier transform spectroscopy with a laser frequency comb," *Nat. Photonics* **3**(2), 99–102 (2009).
7. D. Hillerkuss, R. Schmogrow, T. Schellinger, M. Jordan, M. Winter, G. Huber, T. Vallaitis, R. Bonk, P. Kleinow, F. Frey, M. Roeger, S. Koenig, A. Ludwig, A. Marculescu, J. Li, M. Hoh, M. Dreschmann, J. Meyer, S. Ben Ezra, N. Narkiss, B. Nebendahl, F. Parmigiani, P. Petropoulos, B. Resan, A. Oehler, K. Weingarten, T. Ellermeyer, J. Lutz, M. Moeller, M. Huebner, J. Becker, C. Koos, W. Freude, and J. Leuthold, "26 Tbit s⁻¹ line-rate super-channel transmission utilizing all-optical fast Fourier transform processing," *Nat. Photonics* **5**(6), 364–371 (2011).
8. L. M. Tong, V. D. Miljković, and M. Käll, "Alignment, Rotation, and Spinning Of Single Plasmonic Nanoparticles and Nanowires Using Polarization Dependent Optical Forces," *Nano Lett.* **10**(1), 268–273 (2010).
9. M. Spanner, K. M. Davitt, and M. Y. Ivanov, "Stability of angular confinement and rotational acceleration of a diatomic molecule in an optical centrifuge," *J. Chem. Phys.* **115**(18), 8403–8410 (2001).
10. N. Kanda, T. Higuchi, H. Shimizu, K. Konishi, K. Yoshioka, and M. Kuwata-Gonokami, "The vectorial control of magnetization by light," *Nat Commun* **2**, 362 (2011).
11. G. D. VanWiggeren and R. Roy, "Communication with dynamically fluctuating states of light polarization," *Phys. Rev. Lett.* **88**(9), 097903 (2002).
12. A. Zavyalov, R. Iliew, O. Egorov, and F. Lederer, "Dissipative soliton molecules with independently evolving or flipping phases in mode-locked fiber lasers," *Phys. Rev. A* **80**(4), 043829 (2009).
13. B. Ortaç, A. Zavyalov, C. K. Nielsen, O. Egorov, R. Iliew, J. Limpert, F. Lederer, and A. Tünnermann, "Observation of soliton molecules with independently evolving phase in a mode-locked fiber laser," *Opt. Lett.* **35**(10), 1578–1580 (2010).
14. B. A. Malomed, "Bound Solitons in the Nonlinear Schrödinger-Ginzburg-Landau Equation," *Phys. Rev. A* **44**(10), 6954–6957 (1991).
15. B. A. Malomed, "Bound States of Envelope Solitons," *Phys. Rev. E Stat. Phys. Plasmas Fluids Relat. Interdiscip. Topics* **47**(4), 2874–2880 (1993).
16. N. N. Akhmediev, A. Ankiewicz, and J. Soto-Crespo, "Multisoliton solutions of the complex Ginzburg-Landau equation," *Phys. Rev. Lett.* **79**(21), 4047–4051 (1997).
17. N. N. Akhmediev, A. Ankiewicz, and J. M. Soto-Crespo, "Stable soliton pairs in optical transmission lines and fiber lasers," *J. Opt. Soc. Am. B* **15**(2), 515–523 (1998).
18. P. Grelu, F. Belhache, F. Gutty, and J. M. Soto-Crespo, "Phase-locked soliton pairs in a stretched-pulse fiber laser," *Opt. Lett.* **27**(11), 966–968 (2002).
19. D. Y. Tang, B. Zhao, L. M. Zhao, and H. Y. Tam, "Soliton interaction in a fiber ring laser," *Phys. Rev. E Stat. Nonlin. Soft Matter Phys.* **72**(0), 016616 (2005).

20. B. Zhao, D. Y. Tang, P. Shum, X. Guo, C. Lu, and H. Y. Tam, "Bound twin-pulse solitons in a fiber ring laser," *Phys. Rev. E Stat. Nonlin. Soft Matter Phys.* **70**(6), 067602 (2004).
21. D. Y. Tang, B. Zhao, D. Y. Shen, C. Lu, W. S. Man, and H. Y. Tam, "Compound pulse solitons in a fiber ring laser," *Phys. Rev. A* **68**(1), 013816 (2003).
22. N. H. Seong and D. Y. Kim, "Experimental observation of stable bound solitons in a figure-eight fiber laser," *Opt. Lett.* **27**(15), 1321–1323 (2002).
23. M. J. Guy, D. U. Noske, and J. R. Taylor, "Generation of Femtosecond Soliton Pulses by Passive Mode Locking of an Ytterbium-Erbium Figure-of-eight Fiber Laser," *Opt. Lett.* **18**(17), 1447–1449 (1993).
24. X. Wu, D. Y. Tang, X. N. Luan, and Q. Zhang, "Bound states of solitons in a fiber laser mode locked with carbon nanotube saturable absorber," *Opt. Commun.* **284**(14), 3615–3618 (2011).
25. X. L. Li, S. M. Zhang, Y. C. Meng, Y. P. Hao, H. F. Li, J. Du, and Z. J. Yang, "Observation of soliton bound states in a graphene mode locked erbium-doped fiber laser," *Laser Phys.* **22**(4), 774–777 (2012).
26. L. L. Gui, X. S. Xiao, and C. X. Yang, "Observation of various bound solitons in a carbon-nanotube-based erbium fiber laser," *J. Opt. Soc. Am. B* **30**(1), 158–164 (2013).
27. T. Hasan, Z. P. Sun, F. Q. Wang, F. Bonaccorso, P. H. Tan, A. G. Rozhin, and A. C. Ferrari, "Nanotube-polymer composites for ultrafast photonics," *Adv. Mater.* **21**(38-39), 3874–3899 (2009).
28. F. Wang, A. G. Rozhin, V. Scardaci, Z. Sun, F. Hennrich, I. H. White, W. I. Milne, and A. C. Ferrari, "Wideband-tuneable, nanotube mode-locked, fibre laser," *Nat. Nanotechnol.* **3**(12), 738–742 (2008).
29. Z. Sun, A. G. Rozhin, F. Wang, V. Scardaci, W. I. Milne, I. H. White, F. Hennrich, and A. C. Ferrari, "L-band ultrafast fiber laser mode locked by carbon nanotubes," *Appl. Phys. Lett.* **93**(6), 061114 (2008).
30. A. G. Rozhin, Y. Sakakibara, S. Namiki, M. Tokumoto, H. Kataura, and Y. Achiba, "Sub-200-fs pulsed erbium-doped fiber laser using a carbon nanotube-polyvinylalcohol mode locker," *Appl. Phys. Lett.* **88**(5), 051118 (2006).
31. S. Y. Set, H. Yaguchi, Y. Tanaka, and M. Jablonski, "Laser mode locking using a saturable absorber incorporating carbon nanotubes," *J. Lightwave Technol.* **22**(1), 51–56 (2004).
32. S. Y. Set, H. Yaguchi, Y. Tanaka, and M. Jablonski, "Ultrafast fiber pulsed lasers incorporating carbon nanotubes," *Ieee J Sel Top Quant* **10**(1), 137–146 (2004).
33. Z. Sun, A. G. Rozhin, F. Wang, T. Hasan, D. Popa, W. O'Neill, and A. C. Ferrari, "A compact, high power, ultrafast laser mode-locked by carbon nanotubes," *Appl. Phys. Lett.* **95**(25), 253102 (2009).
34. C. Mou, S. Sergeev, A. Rozhin, and S. Turistyn, "All-fiber polarization locked vector soliton laser using carbon nanotubes," *Opt. Lett.* **36**(19), 3831–3833 (2011).
35. M. Grapinet and P. Grelu, "Vibrating soliton pairs in a mode-locked laser cavity," *Opt. Lett.* **31**(14), 2115–2117 (2006).
36. N. Akhmediev and J. M. Soto-Crespo, "Dynamics of Solitonlike Pulse Propagation in Birefringent Optical Fibers," *Phys. Rev. E Stat. Phys. Plasmas Fluids Relat. Interdiscip. Topics* **49**(6), 5742–5754 (1994).
37. S. V. Sergeev, "Spontaneous light-polarization symmetry breaking for an anisotropic ring-cavity dye laser," *Phys. Rev. A* **59**(5), 3909–3917 (1999).
38. S. Sergeev, "Interplay of an Anisotropy and Orientational Relaxation Processes in Luminescence and Lasing of Dyes," in *Liquid Crystals, Display, and Laser Materials*, H. S. Nalwa, ed. (Academic Press, San Diego, USA, 2001), pp. 247–276.

1. Introduction

Vector solitons (VSs) in mode locked lasers present a train of stabilized short pulses with the specific shape defined by a complex interplay and balance between the effects of gain/loss, dispersion, nonlinearity, and the state of polarization (SOP) either rotating with the period of a few round trips or locked [1–4]. The stability of VSs at the different time scales from femtosecond to microseconds is an important issue to be addressed for increased resolution in metrology [5], high precision spectroscopy [6] and suppressed phase noise in high speed fiber optic communication [7]. In addition, there is considerable interest in achieving high flexibility in the generation and control of dynamic SOPs in the context of trapping and manipulation of atoms and nanoparticles [8, 9], control of magnetization [10], and secure communications [11].

The stability and evolution of vector solitons at a time interval from a few to thousands of cavity round trips is defined by asymptotic states (attractors) which the laser SOP approaches at a long time scale, viz. fixed point, periodic, quasi-periodic, and chaotic one [11]. Solitons can bind together to form a bound state and so, in addition to polarization stability, the stability of bound state in the context of delay and phase shift have to be considered as well [12, 13].

Malomed firstly theoretically predicted the existence of bound state soliton using Ginzburg-Landau equation [14, 15]. It was pointed out that direct soliton interaction can form bound states of solitons with fixed and discrete separations. The bound state solitons also possesses a fixed phase difference i.e. 0 , π , $\pi/2$ [16, 17]. Very recently, bound state solitons

with independently varying phases has been theoretically predicted [12]. To date, bound state solitons have been experimentally observed in various types of passively mode locked fiber lasers including nonlinear polarization rotation (NPR) mode locked fiber laser [18–21] and the figure-of-eight fiber laser [22, 23]. Recently, bound state solitons have been observed in novel carbon nanotubes (CNT) and graphene based mode locked fiber lasers [24–26].

So far, the polarization dynamics of bound state soliton in mode locked lasers has not been studied. Unlike NPR configuration where output is linearly polarized and figure-of-eight configuration where active and passive cavity have to be matched with high precision, CNT polymer composite based mode locked lasers has attracted a lot of attention due to their low cost, ease of fabrication and implementation [27–33]. Most importantly, CNT mode locker does not suffer from polarization sensitivity which inherently extends the possibility of studying polarization dynamics in mode locked lasers. In addition to this, we demonstrate for the first time that CNT polymer composite mode locked laser provides high tunability among different locked and precessing SOPs and between tightly, loosely, interleaved and complex bound states.

2. Experimental set-up

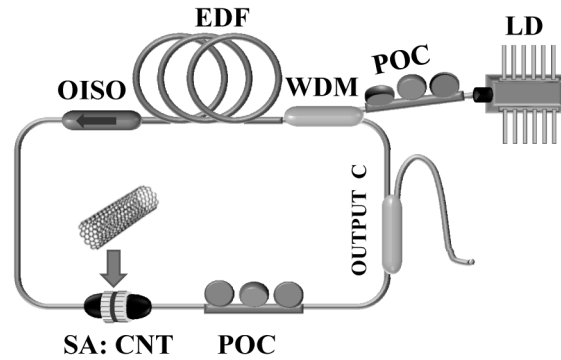


Fig. 1. Experimental set-up.

The experimental setup is shown in Fig. 1. The ring cavity fiber laser with the total length of 7.83 m comprises ~2 m of erbium doped fiber (Liekki Er80-8/125, group velocity dispersion is $\beta_{2,EDF} = -19.26 \text{ ps}^2/\text{km}$.) and standard single mode (SMF-28) fiber with anomalous dispersion, two in-line polarization controllers (PC) and a 980/1550 nm wavelength division multiplexer (WDM). An in-fiber optical isolator is used to maintain unidirectional lasing operation. 90% of the laser light is coupled out of the cavity through a 90:10 fused fiber coupler. The CNT mode-locker is sandwiched between two standard fiber connectors and the index matching gel is applied to minimize the loss. Detailed information regarding the CNT mode locker can be found in [34]. The laser is pumped via the WDM by a fiber grating stabilized 976 nm laser diode (LD) with the maximum current of about 355 mA which provide 170 mW of optical power. The total dispersion of the laser cavity is anomalous which will result in soliton output pulses with typical Kelly side bands. Laser output has been characterized by a commercial autocorrelator (Pulsecheck), an oscilloscope (Tektronix), an optical spectrum analyzer (ANDO AQ6317B) and a commercial polarimeter (Thorlabs, IPM5300). The polarimeter with 1 μs resolution and interval of 1 ms (40 – 40000 round trips) is employed to measure the normalized Stokes parameters s_1 , s_2 , s_3 and degree of polarization (DOP) which are related to the output powers of two linearly cross-polarized SOPs $|\mu|^2$ and $|\nu|^2$, and phase difference between them $\Delta\phi$ as follows:

$$S_0 = |u|^2 + |v|^2, S_1 = |u|^2 - |v|^2, S_2 = 2|u||v|\cos\Delta\phi, S_3 = 2|u||v|\sin\Delta\phi, s_i = \frac{S_i}{\sqrt{S_1^2 + S_2^2 + S_3^2}},$$

$$DOP = \frac{\sqrt{S_1^2 + S_2^2 + S_3^2}}{S_0}, (i = 1, 2, 3)$$

(1)

During the experiment, the pump current has been varied from 240 mA to 355 mA while both intra-cavity polarization and pump polarization control have been implemented to achieve polarization attractors shown in Figs. 2-5. In terms of the sensitivity of the auto-correlator regarding the input SOP, all auto-correlation traces have been averaged over 16 samples.

3. Results and discussion

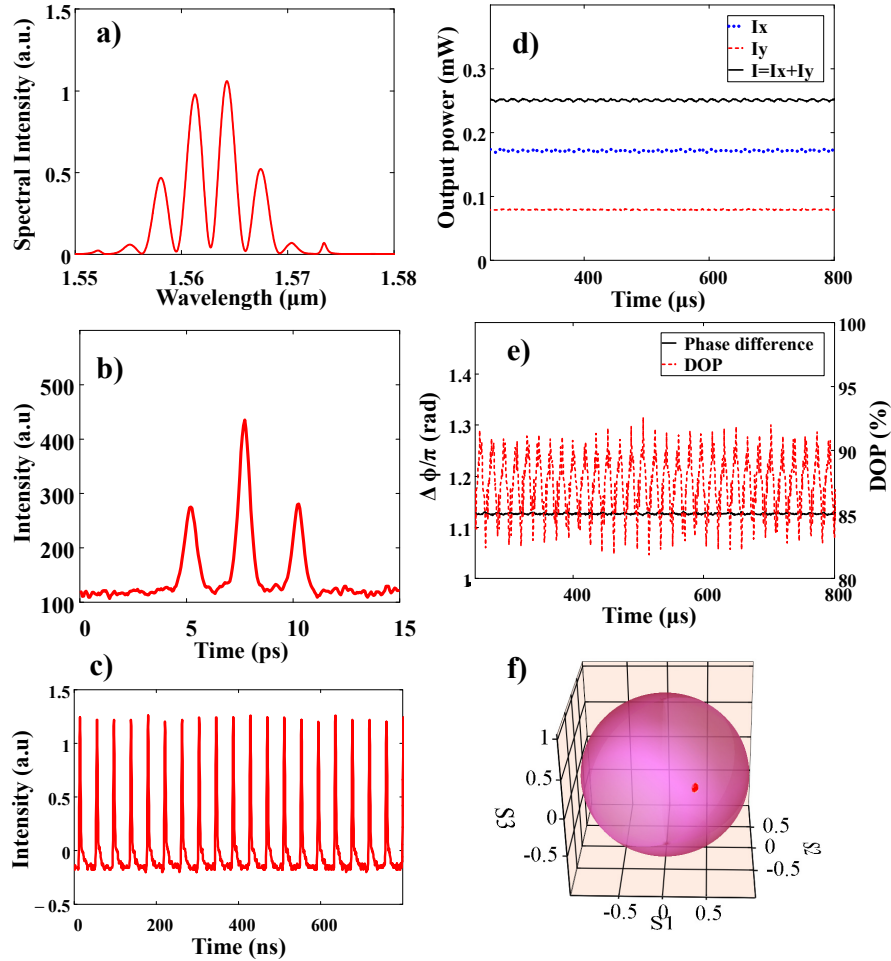


Fig. 2. Polarization locked vector bound state soliton. (a) output optical spectrum, (b) measured auto-correlation trace, (c) single pulse train. Polarization dynamics in the time frame of 40-40 000 round trips (1 μ s – 1 ms) in terms of (d) optical power of orthogonally polarized modes I_x (blue dotted line) and I_y (red dashed line), total power $I = I_x + I_y$ (black solid line), (e) phase difference and degree of polarization, and (f) normalized Stokes parameters at Poincaré sphere. Parameters: pump current $I_p = 240$ mA, period $T = 38.9$ ns, pulse width $T_p = 494$ fs, output power $I = 0.25$ mW, phase difference $\Delta\phi \approx 1.125\pi$.

Figure 2 shows the experimental results for pump current of 240 mA. The output optical spectrum with modulated pattern indicates formation of a two soliton bound state shown in Fig. 2(a). The optical spectrum indicates a π phase difference between the bound solitons [24]. Stable two pulse bound state is characterized by autocorrelation trace shown in Fig. 2(b). Defined by the autocorrelation function, three peaks will appear when two soliton pulses are bound together with a fixed phase difference. The pulse separation is ~ 2.5 ps which is ~ 5 times of the pulse duration (494 fs) indicating tightly bound solitons. The recorded pulse train shows a repetition rate of 25.7 MHz presenting the laser is operating in a single pulse regime. By properly adjusting the PC, the output laser pulse has a fixed SOP with a fixed phase difference $\sim 1.125\pi$ between the orthogonal polarization states which is shown in Figs. 2(d) and 2(e). The output power is ~ 0.25 mW with an averaged DOP of $\sim 90\%$. The high DOP proves

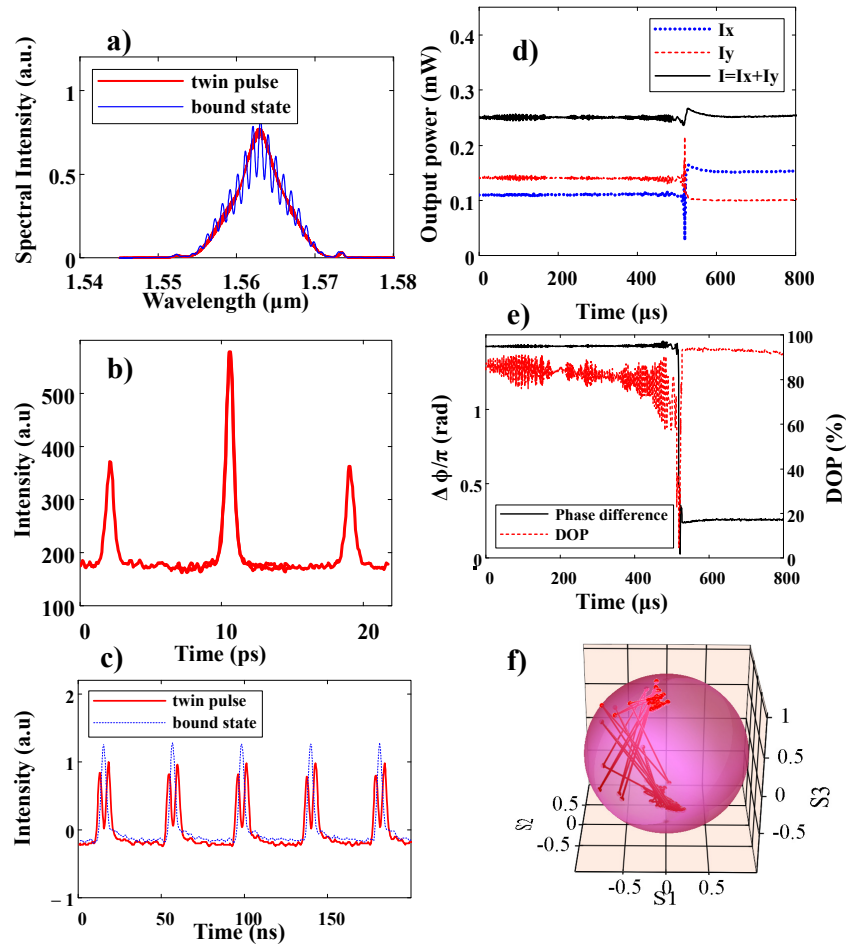


Fig. 3. Vector soliton with slowly evolving state of polarization of bistable operation (a) output optical spectrum of bound soliton (blue solid line) and twin pulse operation (red solid line), (b) measured auto-correlation trace for bound soliton, (c) single pulse train of bound soliton (blue dashed line) and twin pulse operation (red solid line). Polarization dynamics in the time frame of 40-40 000 round trips ($1 \mu\text{s} - 1 \text{ms}$) in terms of (d) optical power of orthogonally polarized modes I_x (blue dotted line) and I_y (red dashed line), total power $I = I_x + I_y$ (black solid line), (e) phase difference and degree of polarization, and (f) normalized Stokes parameters at Poincaré sphere. Parameters: pump current $I_p = 240$ mA, period $T = 38.9$ ns, pulse width $T_p = 494$ fs, output power $I \approx 0.25$ mW.

the vector nature of the soliton bound state in a locked polarization state as shown in Fig. 2(f).

By tuning the PCs, we can achieve bistable operation in the form of switching between bound state soliton (blue lines in Figs. 3(a) and 3(c)) with pulse separation of 10 ps and twin pulse operation with separation of few ns (red lines in Figs. 3(a) and 3(c)). For bound state soliton, pulse separation is oscillating and so fringe contrast in Fig. 3(a) is suppressed [35]. For the twin-pulse operation pulses are uncorrelated and so there are no fringes in optical spectrum (Fig. 3(a)). Therefore, we would only see a single peak autocorrelation trace rather than three peaks. The pulse period is of 38.9 ns, pulse width of 494 fs and output power of 0.25 mW. In view of pulse separation is more than 5 times of pulse width, the bound state soliton satisfies criteria loosely bound state [24]. As shown in Figs. 3(e)-3(f), the bistable operation results in polarization switching between two cross polarized SOPs of particular state, viz. loosely bound state or twin pulse.

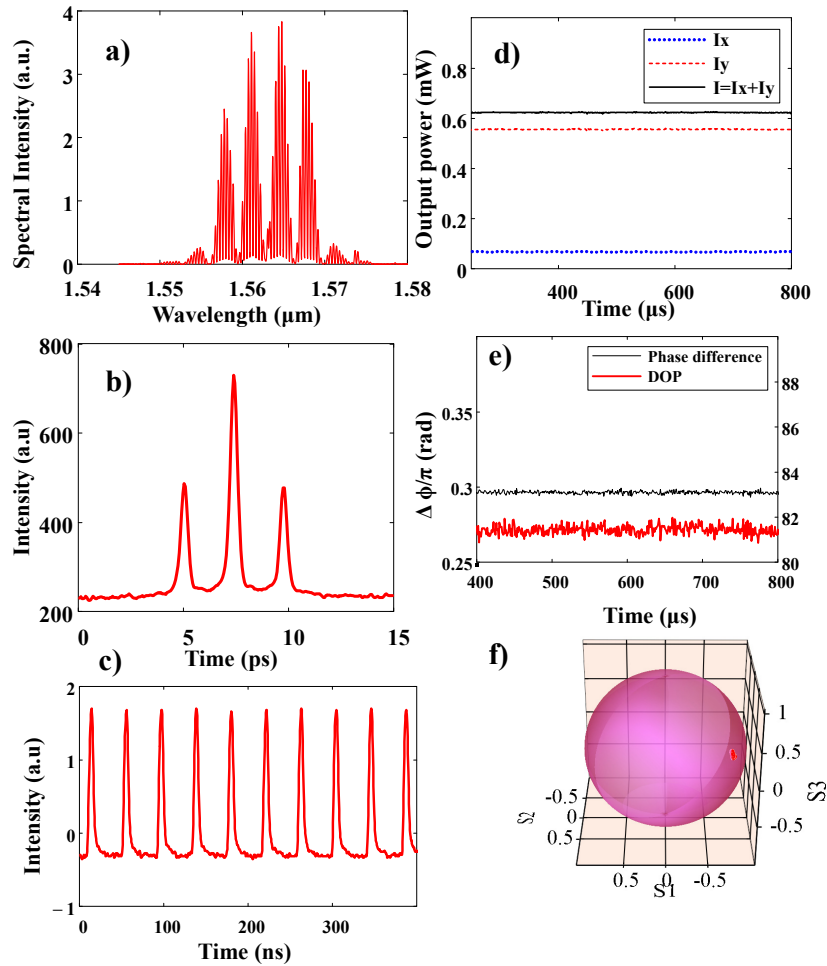


Fig. 4. Vector soliton with slowly evolving state of polarization for multiple bound states operation. (a) output optical spectrum, (b) measured auto-correlation trace, (c) single pulse train. Polarization dynamics in the time frame of 40-40 000 round trips ($1 \mu\text{s} - 1 \text{ms}$) in terms of (d) optical power of orthogonally polarized modes I_x (blue dotted line) and I_y (red dashed line), total power $I = I_x + I_y$ (black solid line), (e) phase difference and degree of polarization, and (f) normalized Stokes parameters at Poincaré sphere. Parameters: pump current $I_p = 320 \text{ mA}$, period $T = 38.9 \text{ ns}$, pulse width $T_p = 383 \text{ fs}$, output power $I = 0.62 \text{ mW}$.

By increasing the pump current to 320mA, we observed an optical spectrum with an additional modulation of spectral fringes (Fig. 4(a)). As follows from [26], spectrum is close to the symmetrical one for low and high frequency fringes and so observed bound state is a two π -shifted bound state complex. Pulse width of 383 fs and the pulse separation of 2 ps (> 5 pulse widths) shown in Fig. 4(b) along with slightly suppressed contrast of fringes in Fig. 4 (a) indicate that solitons in complex are loosely bound [24]. Similar to the bound state operation shown in Fig. 2, bound state complex is polarization locked which is followed by fixed output pulse powers (Fig. 4(d)), fixed phase difference of $\sim 0.3 \pi$, high DOP of $\sim 83\%$ (Fig. 4(e)), and fixed SOP (Fig. 4(f)).

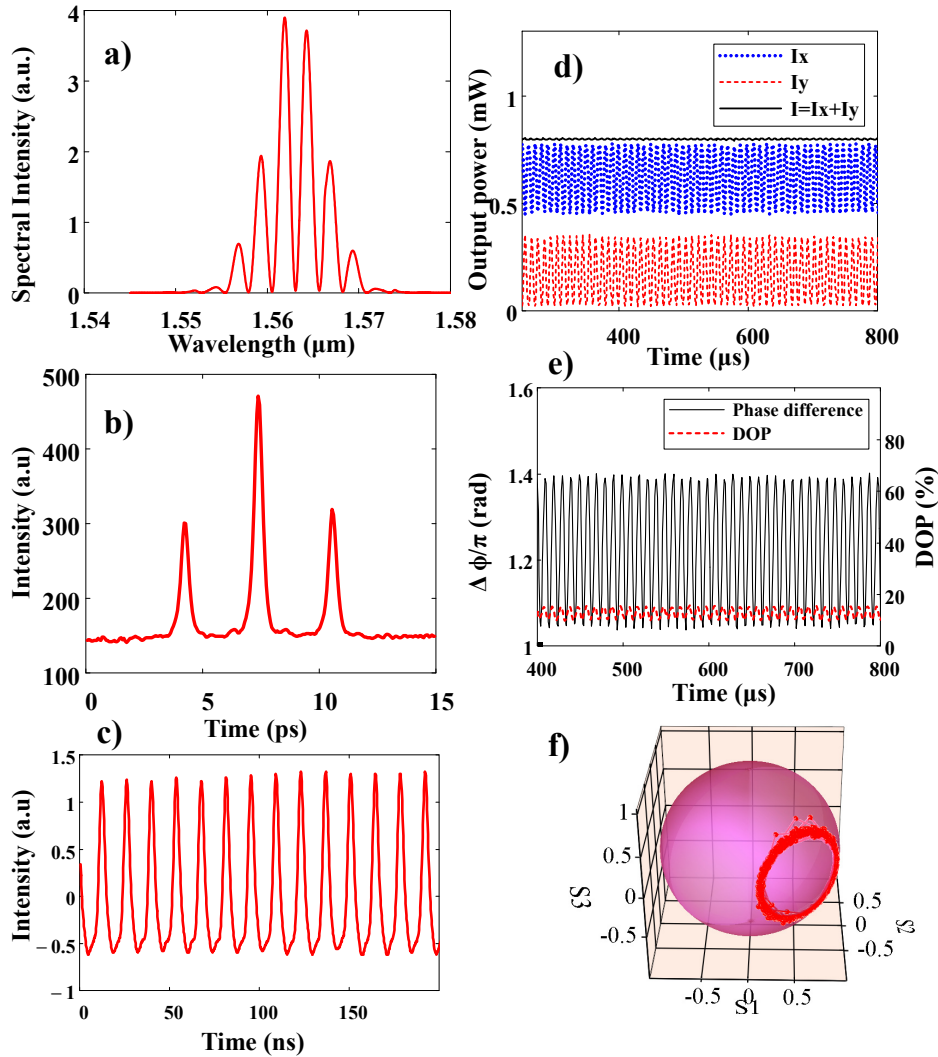


Fig. 5. Vector soliton with slowly evolving state of polarization for three-pulse operation. (a) output optical spectrum, (b) measured auto-correlation trace, (c) single pulse train. Polarization dynamics in the time frame of 40-40 000 round trips ($1 \mu\text{s} - 1 \text{ms}$) in terms of (d) optical power of orthogonally polarized modes I_x (solid line) and I_y (dashed line), total power $I = I_x + I_y$ (dotted line), (e) phase difference and degree of polarization, and (f) normalized Stokes parameters at Poincaré sphere. Parameters: pump current $I_p = 355 \text{ mA}$, period $T = 13 \text{ ns}$, pulse width $T_p = 383 \text{ fs}$, output power $I \approx 0.8 \text{ mW}$.

By further increasing the pump current to 355 mA and tuning the PC, combined harmonic mode locking with bound state soliton is observed with period of 13 ns, pulse width of 383 fs and output power of 0.8 mW (Figs. 5(a)-5(d)). The pulse separation is ~ 3 ps which is ~ 9 times of pulse duration showing loosely bound soliton [24]. The central dip in the spectrum and spectral symmetry illustrates a π phase shift between the two bound solitons [26]. Anti-phase dynamics of oscillation of the orthogonal polarized SOP leads to CW operation of the output pulse (Fig. 5(d)). Different scenarios could lead to the low DOP of 15% as shown in Fig. 5 (e). For example, three bound states solitons can interleave in time with resulting operation at third harmonic shown in Fig. 5(c). Each of bound state can have different SOP and so averaging over 40 round trips results in low DOP shown in Fig. 5(e). The SOP jumps shown in Fig. 5(f) can be considered as an indication of such scenario. To interpret this more rigorously, a polarimeter with a resolution of a pulse round trip is required. An additional cyclic SOP evolution can be explained as follows. As shown by Akhmediev and Soto-Crespo [36], the eigenstates in a fiber in the presence of linear birefringence and circular birefringence caused by nonlinear self-phase modulation are split into two pairs:

$$S^{(1,2)} = \begin{pmatrix} S_0 \\ \pm S_0 \\ 0 \\ 0 \end{pmatrix}, \quad S^{(3,4)} = \begin{pmatrix} S_0 \\ -\alpha \\ 0 \\ \pm \sqrt{S_0^2 - \alpha^2} \end{pmatrix}. \quad (2)$$

Here $S_0 = \text{const}$ and α is determined by the ratio of linear to circular birefringence strength. In mode locked laser, in-cavity polarization controller contributes both into linear and circular birefringence whereas anisotropy induced by pump light is suppressed due to relaxation orientation caused by excitation migration [37, 38]. Mode locked operation changes the active medium anisotropy (both linear and circular) due to polarization hole burning and so the pulse SOP located on a circle as shown in Fig. 5(f). If the beat length in the anisotropic cavity is equal to the round trip and pulse-to-pulse power is constant then pulse SOP is not changed and so vector soliton is polarization locked (Figs. 2(f) and 4(f)). The depth of the hole in orientation distribution of inversion is proportional to the laser power and so with periodical oscillations of the output power (Fig. 5(c)) light induced anisotropy in an active medium will be periodically modulated [37, 38]. If the round trip equals to the rational part of the beat length then SOP after few round trips will slightly deviate from the initial one and can reproduce itself for the period of pulse power oscillations only which is 400 round trips in our case (Fig. 5(f)). Thus, SOP evolution shown in Fig. 5(f) is a superposition of the SOP jumps with precession along the cyclic trajectory on the Poincaré sphere (Fig. 5(f)).

4. Conclusions

Using an in-line polarimeter for erbium doped fiber laser passively mode locked with carbon nanotubes, we demonstrated, for the first time, new types of vector solitons with slowly evolving states of polarization on a time scale of 40-40000 round-trips for tightly, loosely, interleaved and complex bound states. By identifying these new types of unique states of polarization evolving on very complex trajectories, our experimental studies may contribute to new techniques in metrology [5], high-resolution femtosecond spectroscopy [6], high-speed and secure fiber optic communications [7, 11], nano-optics (trapping and manipulation of nanoparticle and atoms [8, 9], and spintronics (vector control of magnetization [10]). It may also open the possibility for creating fundamentally new types of lasers with controlled dynamic states of polarization.

Acknowledgment

Support of the ERC, FP7-PEOPLE-2012-IAPP (project GRIFFON, No 324391) is acknowledged.